A Model Simulation of Air Pollution Over Metro Manila

Mariano A. Estoque[a] and Rochelle Therese F. Balmori[b]*
Climate Studies Division, Manila Observatory
Ateneo de Manila Campus, Loyola Heights
1101 Quezon City, Philippines
P.O. Box 122 U.P. Post Office
1101 Quezon City, Philippines
Tel. No.: (632) 426-5921 to 23; Fax: (632) 426-6141
Email: [a]mae@observatory.ph; [b]rochelle@observatory.ph

ABSTRACT

The diurnal variation of air pollution over Metro Manila is studied by using a theoretical model. The model equations consist of a set of fluid dynamical equations and an equation of mass transport for predicting air pollution. The dynamical equations are based on a mixed layer model of the atmosphere. The source of pollutants is assumed to be uniformly distributed over the Metro Manila area. The source strength varies in time in accordance with the variation of vehicular traffic emission during the day. Model simulations are made in order to determine the effect of varying conditions of the prevailing atmosphere. The results of the simulations indicate a predominantly semi-diurnal variation in the concentration. The maxima usually occur in the early morning and in the evening. This theoretical result is in agreement with long-term averaged observations.

Key words: air pollution, carbon monoxide, numerical modeling, diurnal variation, model simulation

INTRODUCTION

Metro Manila is a highly polluted area, second only to Mexico City which is the most polluted city in the world. According to Kerdar (1996), vehicular traffic is the major source of air pollutants in the area. A study of various pollutants observed during the period of 1975 to 1978 has been made by Valeroso et al. (1996). The area of study is shown in Fig. 1. Valeroso et al. (1996) has shown that in Metro Manila the diurnal variation of the concentrations is predominantly semi-diurnal in nature. A semi-diurnal variation has also been found in Oviedo (Spain) by Garcia et al. (1988). Observations on the average time variation of carbon monoxide for various stations in Metro Manila (Fig. 2) show that the maximum concentrations occur in the morning and in the evening. In contrast, minimum values occur in the early morning and in the early afternoon; the morning minimum is much lower than that in the afternoon. It was also noted that there is a large geographical variation in the magnitude of the concentrations. The largest concentrations were found in Cubao and in Quiapo, and the smallest concentrations were found in Bicutan, which is located in the southern part of Metro Manila. Although the average time variation was basically semi-diurnal, the variations for individual days can be more complicated (Valeroso et al., 1996; Tubal, 2001). Analysis of carbon monoxide and suspended particulate matter (SPM) during a period of several days at two different sites in the Manila Observatory grounds in Quezon City, done through air quality monitoring vans of the National Center for Transportation Studies (NCTS) and the Environmental Management Bureau

* *Corresponding author*

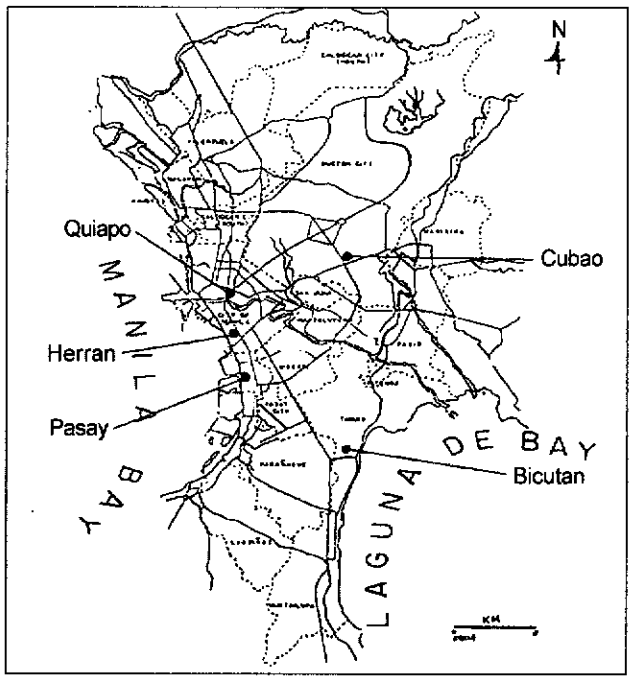

Fig. 1. Map of Metro Manila showing the locations of observational stations (Valeroso et al., 1992).

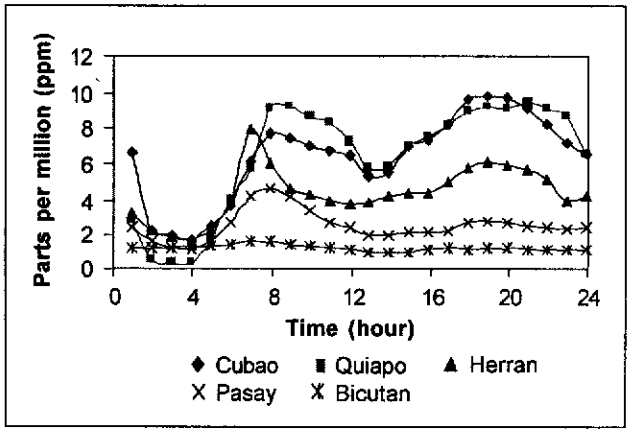

Fig. 2. The average diurnal variation of carbon monoxide (CO) concentrations in Metro Manila (Valeroso et al., 1992).

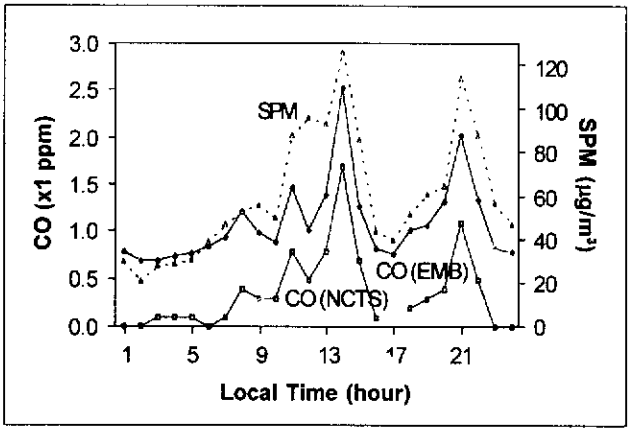

Fig. 3. The diurnal variation of carbon monoxide and suspended particulate matter in the Manila Observatory grounds on May 6, 1999 (Tubal, 2001).

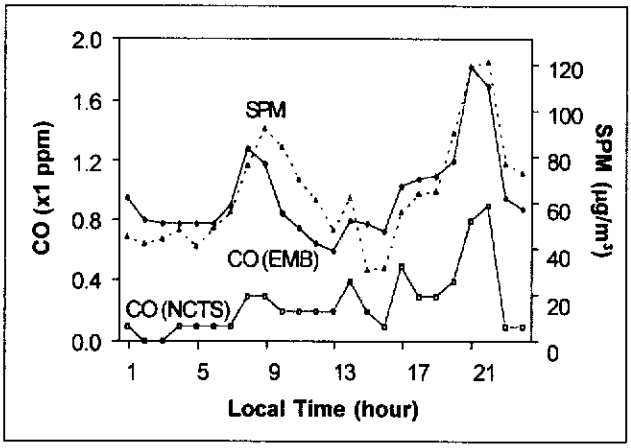

Fig. 4. The diurnal variation of carbon monoxide and suspended particulate matter in the Manila Observatory grounds on May 7, 1999 (Tubal, 2001).

(EMB), also showed diurnal variations for two successive days (May 6 to 7, 1999). The diagram for May 6 (Fig. 3) shows two peaks in the concentrations. One of these peaks occurs near 2:00 P.M., which occurs at a time when the average curves have minimum values, while the other one occurs near 9:00 P.M.. The variations for May 7 (Fig. 4) closely resemble the average curves for May 6. Variations for the other days show much greater deviations from the semi-diurnal variation as shown in the large deviations on May 3, 1999 (Fig. 5). The deviations from the average semi-diurnal variation are presumably due to the effects of sea breezes and other meso-scale disturbances such as topography-induced circulations. These disturbances affect the concentration by changing the height of the mixing layer or inversion height. According to Barkan & Feliks (1993), sea breezes in Israel produce large fluctuations in the inversion height. These disturbances modify the variations of the inversion height due to vertical motions. Variations due to heating are characterized normally by high values near noontime. It can be noted that the three concentration curves (two curves for carbon monoxide and one curve for suspended particulate

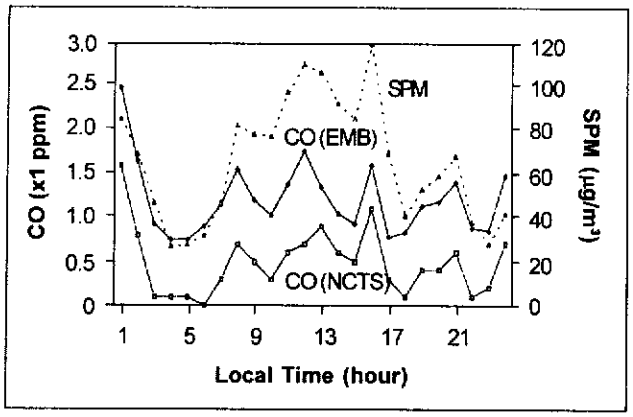

Fig. 5. The diurnal variation of carbon monoxide and suspended particulate matter in the Manila Observatory grounds on May 3, 1999 (Tubal, 2001).

matter) in all of the three diagrams are remarkably very similar in shape. The similarity indicates that the time variations are accurate.

The observed variations of the concentration near the ground described above are essentially due to the varying contributions of three physical processes: horizontal transport or advection, pollutant sources, and sinks. The importance of these processes or factors depends on the characteristics of the prevailing atmospheric condition. The magnitude of the horizontal transport of pollutants depends on the prevailing wind distribution. High wind speeds result in large transports. On the other hand, the effect of the sources on ground concentration depends on the source strength. It also depends on the thermal stratification of the atmosphere. When the atmosphere is stable, the sources produce large concentrations near the ground.

The objective of the present study is to determine the dependence of the concentration patterns on the prevailing atmospheric conditions (wind, cloudiness, and thermal stratification), as well as on the intensity of the pollutant sources and sinks.

METHODOLOGY

The objective of the study is achieved by conducting numerical experiments or simulations with the aid of a theoretical model. In these experiments, we used different prevailing atmospheric conditions to determine the effects of these conditions on the pollution patterns.

Description of the model

The model equations consist of a transport-diffusion equation for pollutant concentration—an equation to predict ground temperature and a set of fluid dynamical equations. The dynamical equations predict the wind and other meteorological variables; these are used in the solution of the transport-diffusion equation. The dynamical equations are based on the so-called "mixed layer model" of the atmosphere. The locations of the observational stations have been based on the work of Valeroso et al. (1996).

The mixed layer model has been used previously to study various types of atmospheric phenomena. One of the earliest applications of the model was made by Lavoie (1972). He used the model to study the effects of Lake Ontario on cold air outbreaks. Later applications were done by other investigators, such as Keyser & Anthes (1977), Estoque & Ninomiya (1976), and Glendening (1990). The study of Glendening is quite pertinent to the present study because he used the model to investigate the sea breeze over the Los Angeles area with some degree of success. In this connection, one notes that the sea breeze circulation, as well as meso-scale circulations generated by the mountains, are important in determining the patterns of pollution over the Metro Manila area.

The mixed layer equations are derived by assuming that the atmosphere has the simple vertical structure shown in Fig. 6. The diagram shows that the complex vertical structure of the real atmosphere is replaced by three layers. The primary layer is the mixed layer. The height of this layer (Z_i) could vary from a few meters to a few kilometers. The mixed layer serves as a depository of atmospheric properties, such as momentum, heat, and pollutants. These are transported upward or downward from the ground. The wind and the potential temperature are assumed constant along the vertical direction in this layer. In

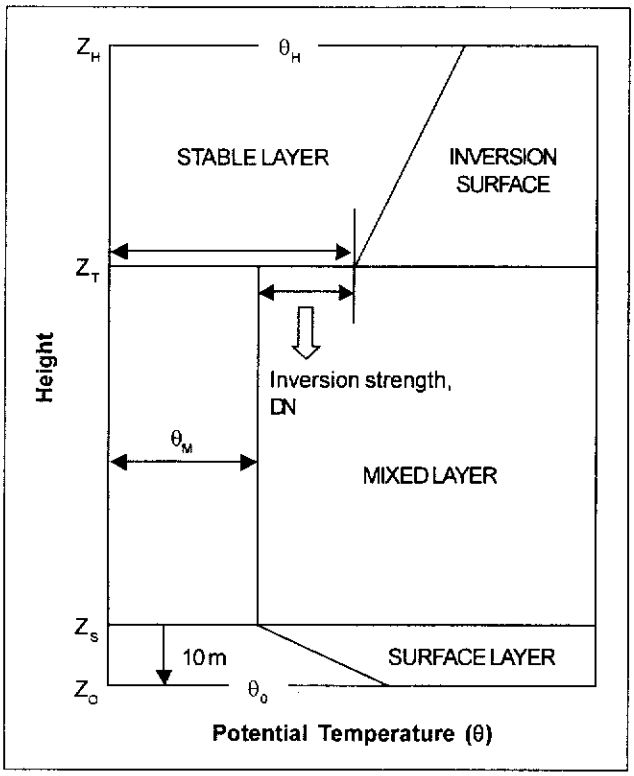

Fig. 6. Vertical temperature structure of the mixed layer model.

the figure, we define the temperature of the base of the inversion as equal to the mixed layer temperature q_M; furthermore, q_H is arbitrarily defined as the temperature of the top of the inversion. The lowest layer, the surface layer, serves as a medium through which heat and momentum are transported from the earth surface to the atmosphere. This layer is introduced in order to simplify the estimation of the vertical fluxes of properties to and from the ground. The base of the surface layer is always assumed to be at the ground for all terrain elevations. The top layer, which is a stable layer, provides a lid to the atmosphere. This layer represents the main bulk of the atmosphere. It is relatively inactive. The temperature lapse rate of the stable layer is assumed to be 6°C per kilometer. The mixed layer equations are relatively well known from previous references such as those cited above. Therefore, for the sake of brevity, we will not discuss their derivation nor write the equations here.

The transport-diffusion equation is based on the box model described by Heinsohn & Kabel (1999). The equation is basically a mass conservation equation applied to a box of the mixing layer whose bottom is the earth surface and whose top is the upper boundary of the mixed layer. The transport-diffusion equation is:

$$\frac{\partial c}{\partial t} = -u\left(\frac{\partial c}{\partial x}\right) - v\left(\frac{\partial c}{\partial y}\right) + K\left(\frac{\partial^2 c}{\partial x^2} + \frac{\partial^2 c}{\partial y^2}\right) + \frac{s}{Z_T} - kc$$

where:

c	is the pollutant concentration;
x, y	are the Cartesian coordinates along the east-west and the north-south directions;
u	is the x component of the wind;
v	is the y component of the wind;
K	is the diffusion coefficient;
s	is the source strength;
Z_T	is the inversion height;
k	is the chemical reaction rate constant; and,
t	is the time

In this initial study, we assume that in Metro Manila the pollutant source strength is constant spatially; however, it varies temporally. The time variation (Fig. 7) is based on the variation of vehicular traffic in Metro Manila according to Kerdar (1996). The magnitude of the source strength has been arbitrarily adjusted so that the resulting concentrations in the model are similar to the observed values.

The sink term is formulated in terms of a first order chemical reaction rate with rate constant k. The rate constant used in this study is based on a value given by Nazaroff & Alvarez-Cohen (2000). The use of this value in the model gives reasonable results.

The surface temperature is predicted by the so-called "force-restore equation", which has been described by Deardorff (1978) and others. The soil parameters, which are used in the equation, have been specified in order to give reasonable surface temperatures. The soil parameters, as well as other environmental parameters, are assumed not to vary with time. Also, for simplicity, in this initial study we assume that the surface temperature is not affected by rainfall and cloudiness. Furthermore, the cleansing effect of rainfall on pollutants is not considered. Future studies will incorporate these effects.

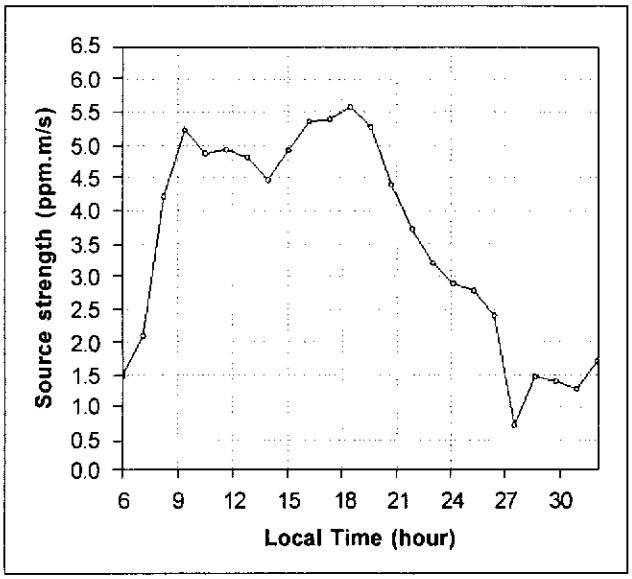

Fig. 7. The time variation of the source strength.

We summarize the description of the model by indicating the important dependent variables which include horizontal wind components (u and v); mixed layer height (Z_i); potential temperature (q); and pollution concentration (c). The independent variables are the two horizontal coordinates (x and y) and time (t).

Numerical integration, boundary conditions, and initial conditions

The equations are integrated numerically for the domain shown in Fig. 8. Metro Manila is the source area for pollutants in the model, as indicated by the shaded portion in the figure. The domain has 42 grid points along the x-axis and 30 grid points along the y-axis. The grid distance is 5 km. The local terrain is incorporated in the model by using a terrain-following system for the vertical coordinate. Finite differencing is done using the forward upstream differencing scheme. Lateral boundary values are held constant except at outflow points. At any one of these points, the boundary value is specified as equal to the value at the adjacent interior point upstream. The initial time for all numerical integrations correspond to 6:00 A.M. (local time). The important variables which are specified at this time, are the mixed layer values of the wind components (u and v), potential temperature (q), the mixed layer height, and the pollutant concentration (c).

In addition to these variables, we also specify the initial ground temperature. The initial values of the mixed layer potential temperature and the ground temperature are specified to be equal to the sea surface temperature (300 K). The initial distribution value of the concentration is horizontally uniform at 0.9 ppm.

Design of the numerical experiments

In order to achieve our goal of determining the dependence of the air pollution patterns on the prevailing atmospheric conditions, we designed several sets of numerical experiments or simulations. The initial values are based on the prevailing conditions. The conditions considered are the wind speed and direction; the strength of inversion; the height of inversion; and cloudiness. Cloudiness determines the intensity of the short-wave radiation reaching the ground. The strength of inversion is defined in this study as the difference between the temperature of the mixed layer and the temperature of the base of the overlying stable layer. This is the quantity DTN, shown in Fig. 6.

All the studies mentioned in the description of the model section, which used the mixed-layer model, specify the strength of the inversion, DTN. The method of specification is based on a replacement of the observed temperature sounding by a mixed-layer sounding. The

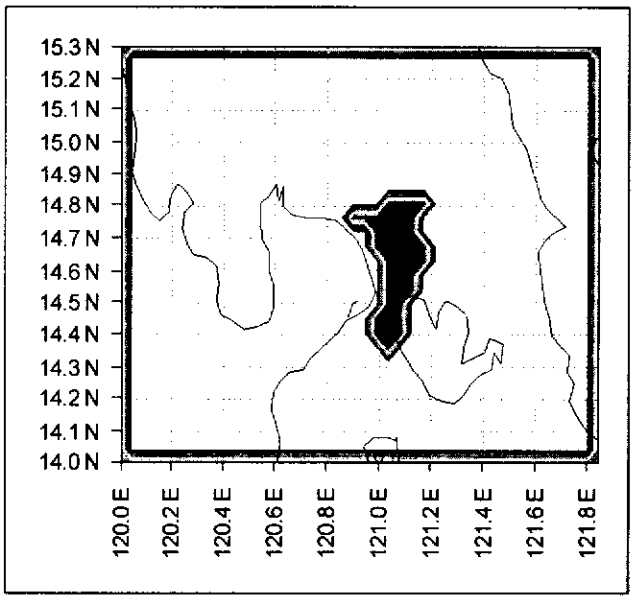

Fig. 8. The computational grid for the experiment.

Table 1. Several numerical experiments done for the study.

Experiment No.	Wind speed (m/s)	Wind direction	Mixed layer height (m)	Inversion strength (DTN, °C)	Cloudiness
1	0.01	SW	200	1	partly cloudy
2a	5.00	SW	200	1	partly cloudy
2b	10.00	SW	200	1	partly cloudy
2c	5.00	NE	200	1	partly cloudy
2d	10.00	NE	200	1	partly cloudy
3a	0.01	SW	300	1	partly cloudy
3b	0.01	SW	500	1	partly cloudy
4	0.01	SW	200	5	overcast
5a	0.01	SW	200	1	overcast
5b	0.01	SW	200	1	cloudy

temperature observations can be made by using radiosondes or by LIDAR. The intensity of the short-wave radiation is specified by assigning appropriate values of the albedo (reflection due to clouds and the ground) in the surface temperature equation.

The numerical experiments are summarized in Table 1. For convenience in discussing the results, we have designated Expt. 1 as the control run. Since the prevailing wind for the control case is 0.01 m/s, we can consider that the wind is essentially calm. The results of other experiments are then compared with those of the control experiment in order to determine the effect of the different parameters associated with the prevailing atmospheric conditions. These parameters are conveniently indicated by numbering the experiments as follows:

Expts. 2a to 2d:	Effect of prevailing wind;
Expts. 3a & 3b:	Effect of mixed layer height;
Expt. 4:	Effect of inversion strength; and
Expts. 5a to 5b:	Effect of cloudiness

RESULTS

Control experiment

Geographical distributions of the wind and pollution concentration

In order to provide a general background for a detailed discussion of the diurnal variations, we describe first the time evolution of the geographical distributions of the pollution concentration for the control experiment. The evolution during the day is indicated in Figs. 9 to 15. Fig. 9 shows the concentration in the morning (9:00 A.M.), just three hours after the initial time. It can be seen that the concentration is essentially constant (3 ppm) over the entire Metro Manila area, which is consistent with the initially uniform concentration pattern and source strength over the area that is assumed at 6:00 A.M.; however, the concentration at 9:00 A.M. is greater than at 6:00 A.M. In addition to the

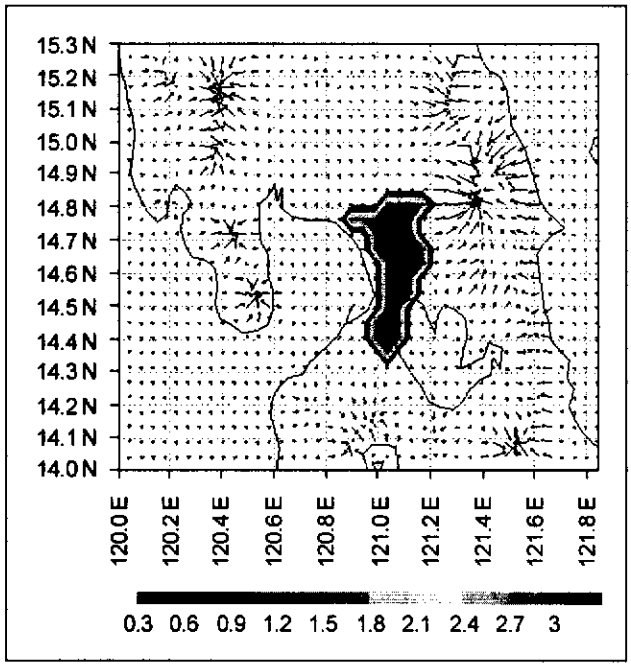

Fig. 9. Geographical distribution of air pollution concentration and wind at 9:00 A.M.. White region indicates concentration less than 0.3 ppm.

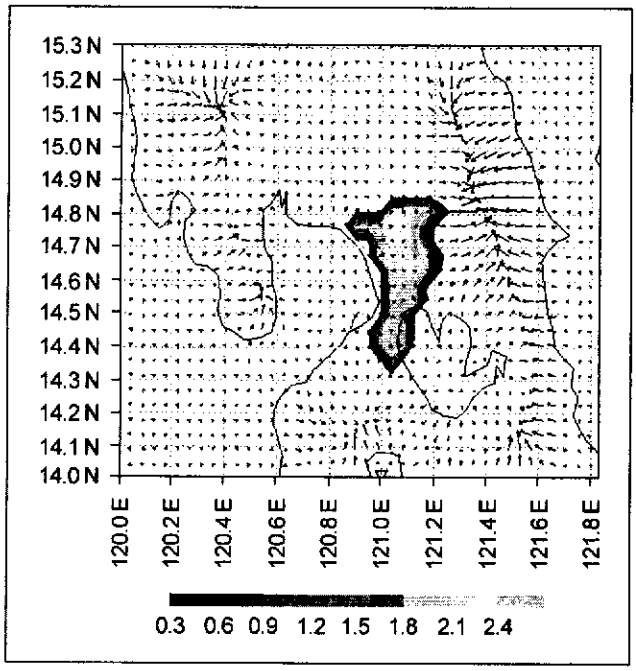

Fig. 10. Geographical distribution of air pollution concentration and wind at 12:00 noon. White region indicates concentration less than 0.3 ppm.

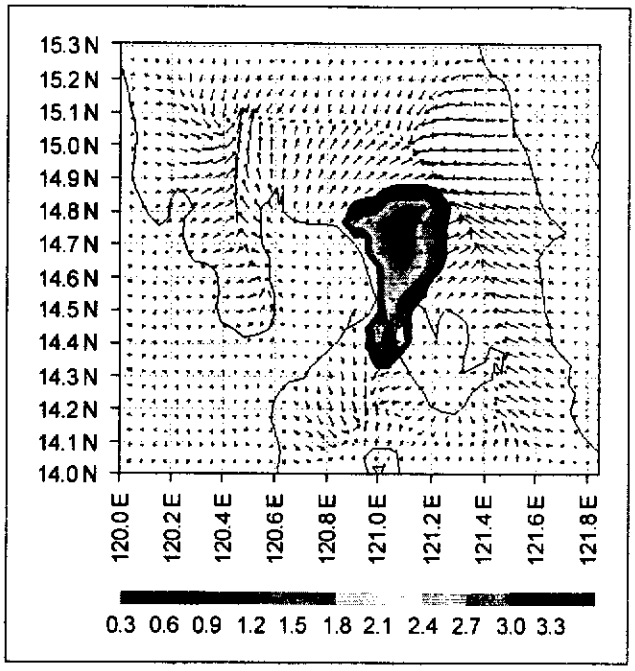

Fig. 12. Geographical distribution of air pollution concentration and wind at 6:00 P.M.. White region indicates concentration less than 0.3 ppm.

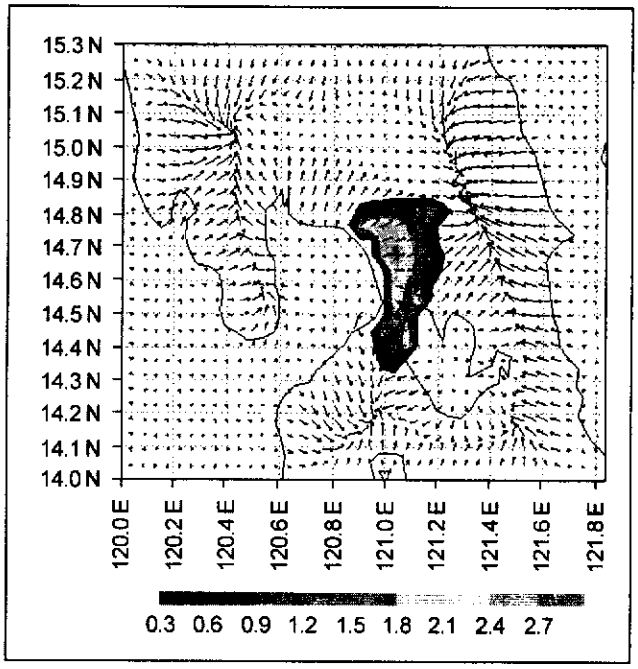

Fig. 11. Geographical distribution of air pollution concentration and wind at 3:00 P.M.. White region indicates concentration less than 0.3 ppm.

concentration, the figure also shows the surface wind distributions. Note the slope winds which developed in the vicinity of the Sierra Madre Mountains, east of Metro Manila. The concentration three hours later at 12:00 noon (Fig. 10) shows a general decrease in the values of the concentration from the previous value of 3 ppm at 9:00 A.M.; the maximum value is now about 2.4 ppm at noontime. The low concentrations at this time are presumably due to the greater mixing heights at this time of the day. Furthermore, significant non-uniformities in the geographical distribution of pollution concentration have developed.

Concentrations over the southern Metro Manila have become generally smaller compared to those of northern Metro Manila. These non-uniformities are the effects of the meso-scale circulations which have been generated by the solar heating of the ground. During the following 6-hour period, the concentrations progressively increase with time as shown in Figs. 11 & 12. The increase in pollution concentration is due to a decrease in the inversion height, together with an increase in the source strength. There is also a slight eastward movement of pollution over the northern part of Metro Manila. This movement is due to the transport of pollution by the northeastward winds associated with sea breeze and slope winds.

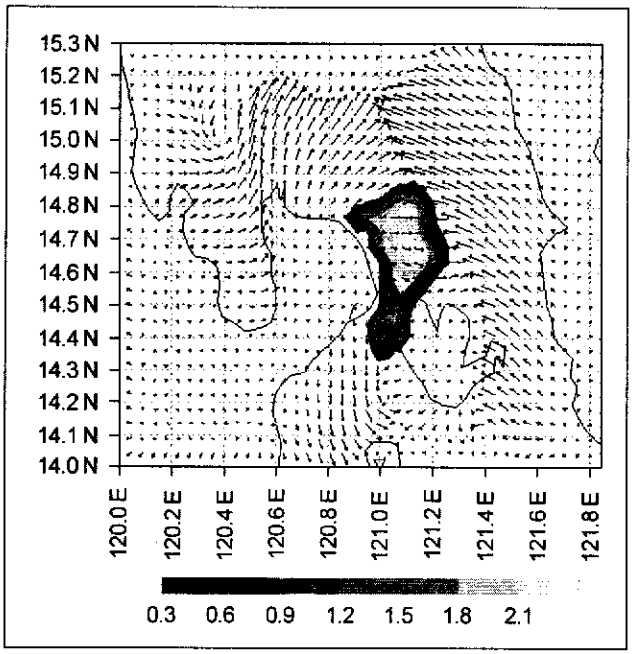

Fig. 13. Geographical distribution of air pollution concentration and wind at 9:00 P.M.. White region indicates concentration less than 0.3 ppm.

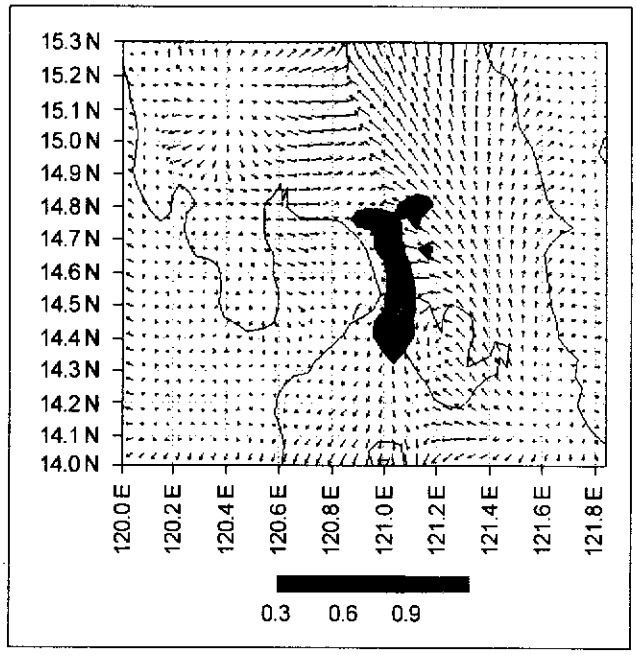

Fig. 15. Geographical distribution of air pollution concentration and wind at 3:00 A.M.. White region indicates concentration less than 0.3 ppm.

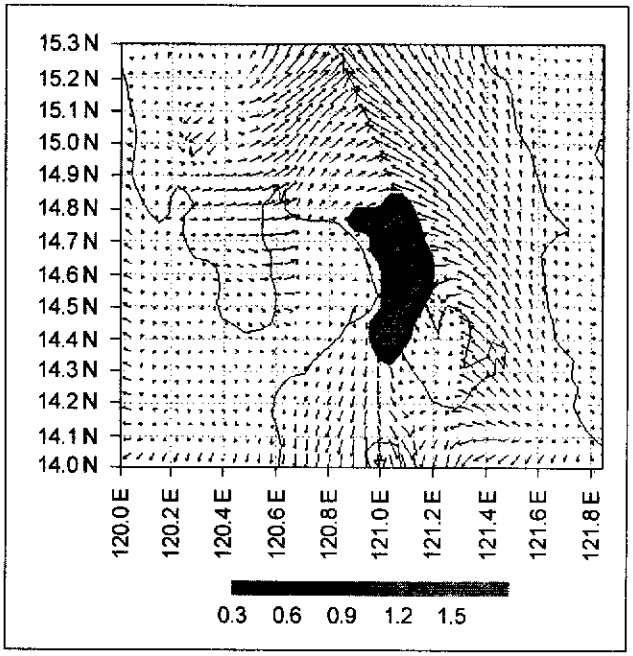

Fig. 14. Geographical distribution of air pollution concentration and wind at 12 midnight. White region indicates concentration less than 0.3 ppm.

The concentrations over southern Metro Manila continue to be relatively low. A possible explanation for the low concentrations in this area is due to the transport of clean air from Manila Bay and Laguna de Bay. After reaching maximum values in the early evening (Fig. 12), the concentrations subsequently decrease as shown in Figs. 13 & 14. This is due to the decrease in the pollution source strength at night. Subsequently, another factor contributes to the low concentrations, especially over the eastern sections of Metro Manila—the movement of a line of high inversion heights from the east. The line is associated with a convergence line which is formed earlier over the Sierra Madre Mountains, located east of Metro Manila. The convergence line develops as a result of the landward extension of the sea breeze from Manila Bay and from the Pacific Ocean. The sea breeze circulations are also reinforced by slope winds, which develop over the Sierra Madre Mountains. The formation and the movement of the convergence line are indicated by the wind patterns in Figs. 12 to 15. The distortion of the shape of the polluted area can be noted as the convergence line moves westward over eastern Metro Manila. This effect is seen clearly by comparing the pollution patterns at 12:00 midnight and at 3:00 A.M. (Figs. 14 & 15).

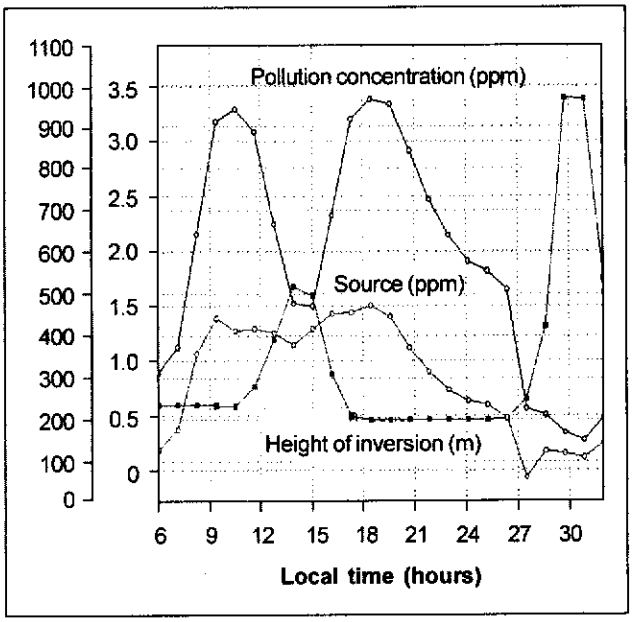

Fig. 16. Relationship of pollution concentration with source strength and height of inversion. Pollution concentration and source are in ppm while height of inversion is in meters.

Diurnal variations of the pollution concentration

We continue the discussion of the results by a more detailed examination of the variations of the pollution concentration during the day. We begin this discussion by looking at Fig. 16, which shows the variations in concentration occuring at a location near the middle of the northern half of the Metro Manila area (longitude = 121.05°E, latitude = 14.75°N). The figure also shows the corresponding variations in the source strength and the height of the mixed layer. These two quantities are important in determining the variation of the concentration when the prevailing wind is weak. It can be seen that the concentration curve shows two peaks: one occurs in the morning, while the other occurs in the early evening. There are two minima: one occurs near noontime, while the other occurs in the early morning. The semi-diurnal variation in the concentration is remarkably similar to the observed variations in Figs. 2 & 4.

The physical processes, which are responsible for the concentration variation shown in Fig. 16, may be explained by the variations in the source strength and the inversion height through the fourth and fifth terms of Eq. (1). The morning peak is primarily the result of the low inversion height at this time of the day. The low inversion confines the pollutant, which is discharged within a thin layer of the atmosphere, resulting in a high concentration. The rapid increase in the rate of pollutant discharge during the same period contributes to a correspondingly rapid increase in the concentration. The relative minimum, which follows at noon, is due primarily to the concomitant maximum in the inversion height. The small decrease in the source strength during the same period could also contribute slightly to the noontime minimum. The sudden increase in the height of inversion from 3:00 A.M. to a peak at 6:00 A.M. is due to the presence of a region of convergence over the area during these times.

In order to describe conveniently the dependence of the diurnal variations on geographical location, we use Hovmoller charts. The abscissa of these charts is a space coordinate (x or y) while the ordinate is time (t). The first chart, Fig. 17, depicts the distribution of concentration at the constant latitude of 14.75°N for varying x (or longitude) and time. There are two

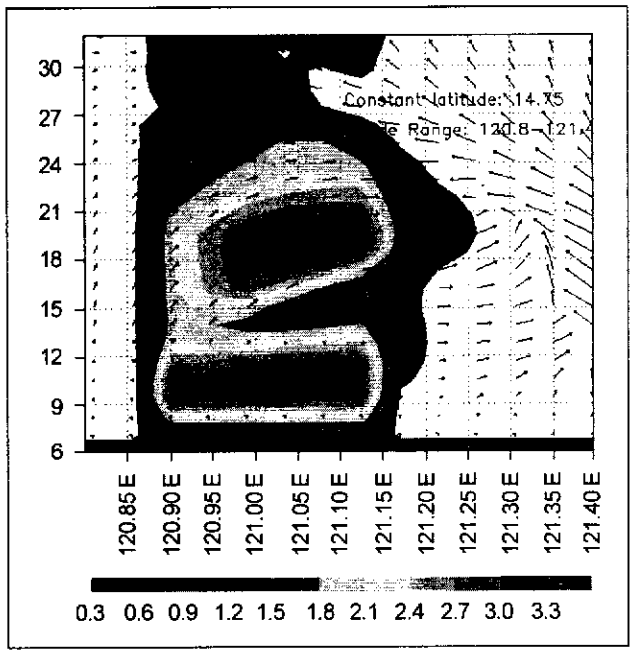

Fig. 17. Hovmoller chart showing the variation of the concentration with time and longitude at 14.75°N for the control case. White region indicates concentration less than 0.3 ppm.

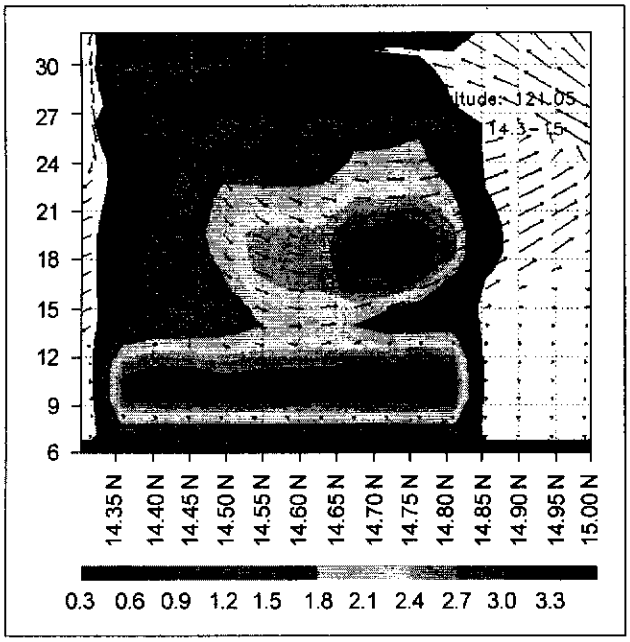

Fig. 18. Hovmoller chart showing the variation of the concentration with time and latitude at 121.05°E for the control case. White region indicates concentration less than 0.3 ppm.

maxima: one in the morning and the other in the evening. The relative minimum between these two maxima occurs in the afternoon. Note that the second maximum (the evening maximum) occurs later in the eastern sectors of Metro Manila. The value of this maximum is smaller in the western sectors. This is probably due to the transport of less polluted air from Manila Bay as indicated in the figure by winds with eastward components. These eastward components cause the extension of the evening maximum toward the east. The next chart, Fig. 18, shows the corresponding concentration and wind distribution as functions of latitude and time at the constant longitude of 121.05°E. This chart also shows the general occurrence of a morning and an evening maximum in the concentration. It can be noted that there is a tendency for a weaker maximum to occur in the evening at lower latitudes or in the southern part of Metro Manila. The weaker evening maximum is in agreement with the observed weaker maximum for the southern station of Pasay in Fig. 2. The weaker maximum appears to be associated with the relatively strong northwest and west winds, which develop in the evening, and transport less polluted air from Manila Bay to the station.

In summary, the two Hovmoller charts (Figs. 17 & 18) show that there are significant geographical variations in the diurnal patterns in pollution concentration. The evening maximum tends to be weaker in the western and the southern sections of Metro Manila. Furthermore, the evening maximum tends to occur earlier in western sections.

Dependence of the diurnal variations on the prevailing atmospheric conditions

We now discuss the effect of the prevailing conditions on the characteristics of the prevailing large-scale atmospheric conditions. The prevailing conditions considered are the wind, mixed layer height, inversion strength, and cloudiness. These conditions were incorporated in the model by specifying them in the initial conditions.

Effect of the prevailing wind

Several simulations or experiments were done to determine the effect of the prevailing wind, but only four of them are presented in this paper. Each experiment is different from one another only in the type of prevailing wind. Thus, by comparing the results of the different experiments with the control case where the prevailing wind is practically calm, one can deduce the dependence of the diurnal variation on the prevailing wind. Two different wind directions are considered: southwest (SW) and northeast (NE). These directions are chosen because they represent the two predominant monsoonal wind directions over Metro Manila. For each wind direction, we consider two wind speeds: moderate (5 m/s) and strong (10 m/s). Hence, there are a total of four simulations presented for this case.

The results of the simulations are shown in the Hovmoller charts of Figs. 19 to 26. Comparing these charts with the corresponding charts for calm prevailing wind in Figs. 17 & 18 shows that the concentrations are much lower in the cases of moderate and strong winds. In general, all these cases tend to have a semi-diurnal variation with a morning, as well as an evening, maximum. Moreover, the amplitudes of the semi-diurnal variations are smaller. The amplitudes are smallest in

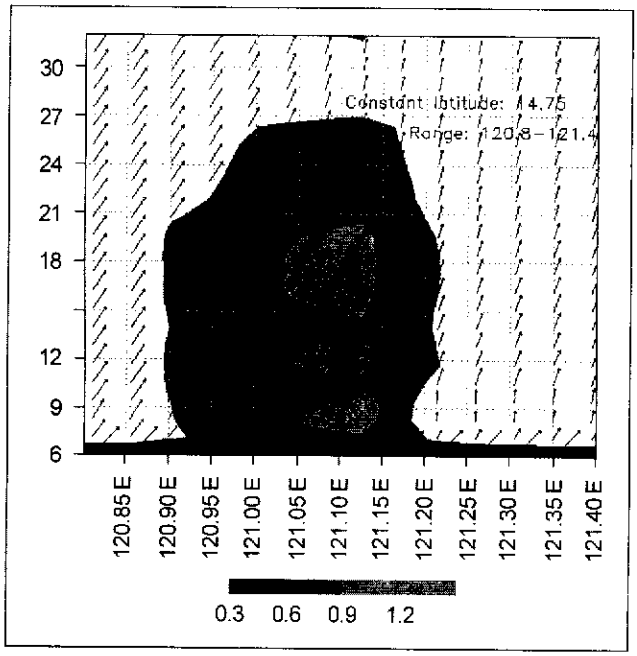

Fig. 19. Hovmoller chart showing the variation of the concentration with time and longitude at 14.75°N latitude. Case: Strong southwest winds. White region indicates concentration less than 0.3 ppm.

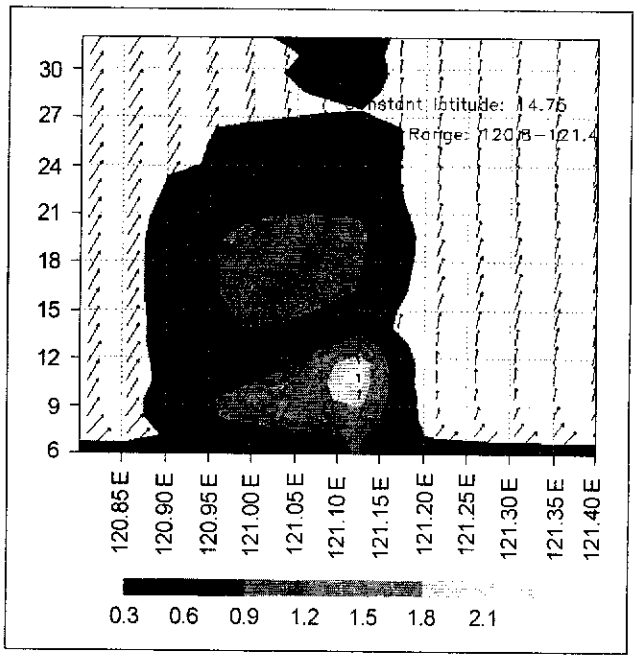

Fig. 20. Hovmoller chart showing the variation of the concentration with time and longitude at 14.75°N latitude. Case: Moderate southwest winds. White region indicates concentration less than 0.3 ppm.

the cases of strong prevailing winds. In almost all the cases, the morning maximum tends to be greater than

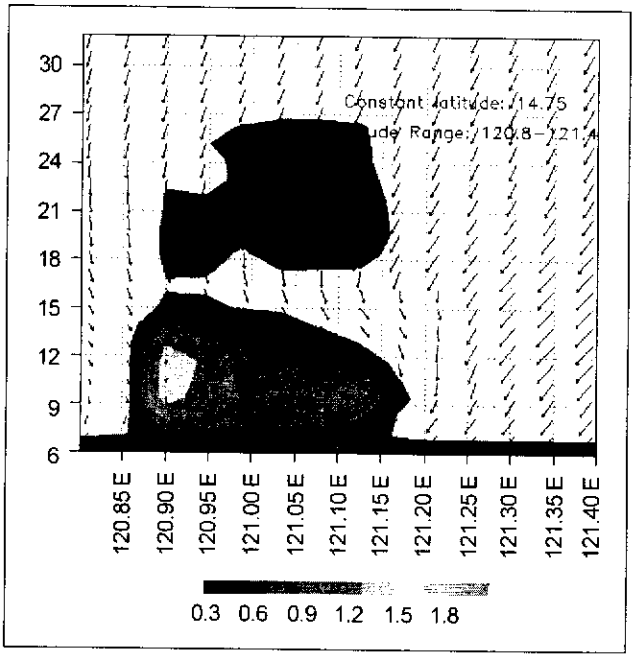

Fig. 21. Hovmoller chart showing the variation of the concentration with time and longitude at 14.75°N latitude. Case: Moderate northeast winds. White region indicates concentration less than 0.3 ppm.

the evening maximum. This is clearly seen in Figs. 20, 21, and 25. Note also that if the wind is from the southwest, the strongest morning maximum occurs over the eastern sections of Metro Manila (Figs. 19 & 20). Conversely, if the wind is from the northeast, the strongest morning maximum occurs over the western sections (Figs. 21 & 22). These distributions for pollutant concentration are obviously due to the effects of horizontal (westward) transport or advection of the pollutant. A similar effect is seen in the latitude-time Hovmoller charts of Figs. 25 & 26. Here, the advection creates a pattern where the morning maximum occurs in the southern part of Metro Manila. In Fig. 25, we also note that there is practically no evening maximum.

In the case of strong northeast winds, Figs. 22 & 26 show that many sections in Metro Manila are virtually pollution-free near noontime. This is associated with the high mixing layer which develops as a result of meso-scale upward motions.

Another interesting pattern is the case with moderate southwest winds in Fig. 24. Here we see that the evening maximum occurs only over the southern and the northern sections of Metro Manila. In the central

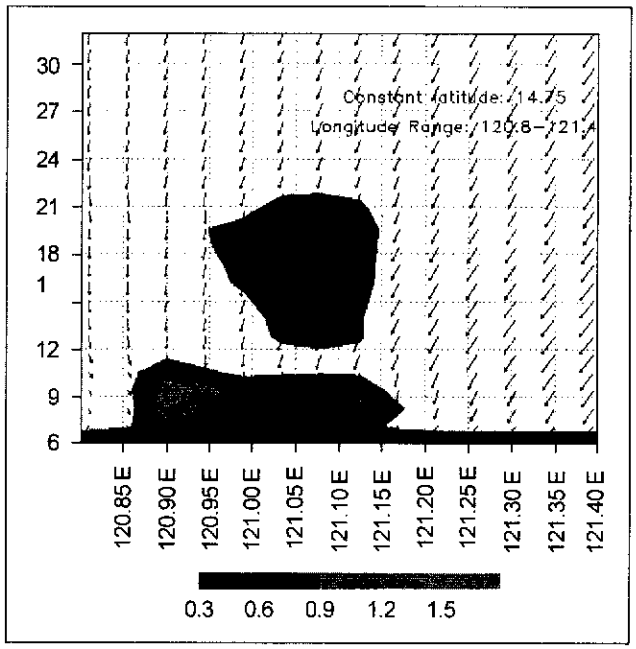

Fig. 22. Hovmoller chart showing the variation of the concentration with time and longitude at 14.75°N latitude. Case: Strong northeast winds. White region indicates concentration less than 0.3 ppm.

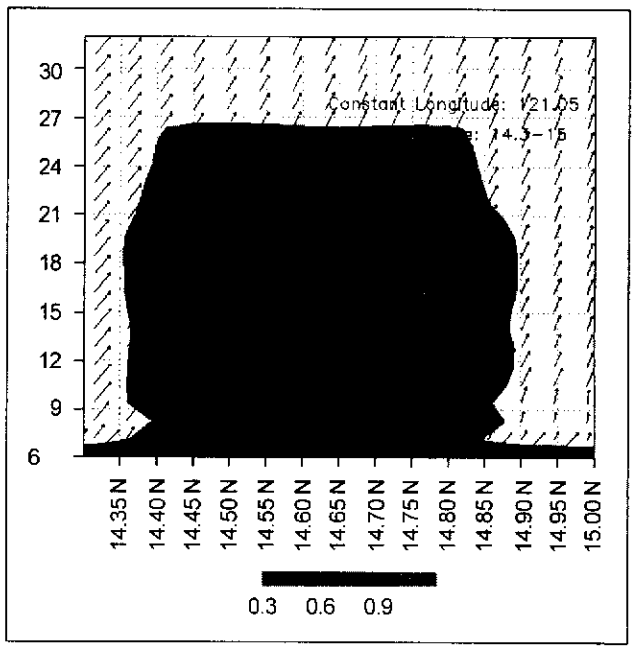

Fig. 23. Hovmoller chart showing the variation of the concentration with time and latitude at 121.05°E longitude. Case: Strong southwest winds. White region indicates concentration less than 0.3 ppm.

section, the diurnal variation has practically only one maximum. Finally, we note the interesting variation in Fig. 19 which shows three maxima: one in the morning, another at noon, and still another in the early evening.

In summary, we find that there are large differences in the diurnal variation which are associated with different prevailing winds. Nevertheless, there is a strong tendency for the variations to have a morning, as well as an evening, maximum.

Effect of cloudiness

Cloudiness affects the amount of the solar radiation reaching the ground. The amount of solar radiation, in turn, determines the degree of heating of the ground and the increase of the ground temperature during daytime. The heating of the ground affects the concentration mainly because of its effect in changing the height of the mixed layer. The height of inversion is affected in two ways: first, the height increases as a result of the flux of heat from the ground; and secondly, the heating results in horizontal temperature gradients and the subsequent development of meso-scale circulations such as the sea

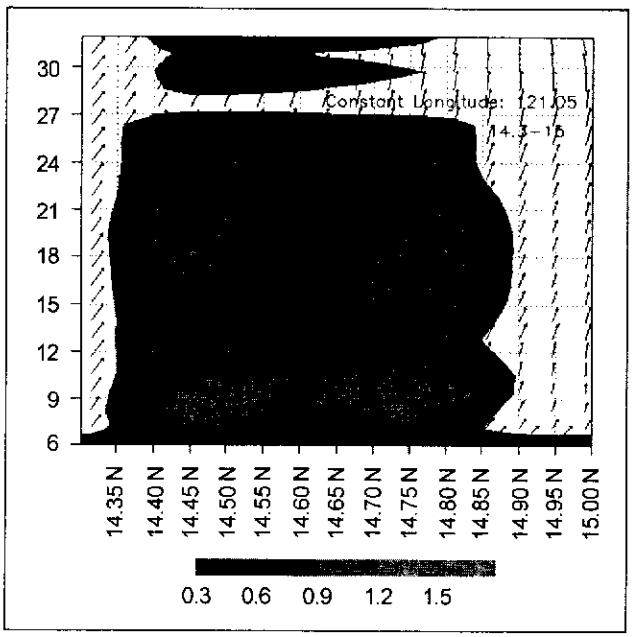

Fig. 24. Hovmoller chart showing the variation of the concentration with time and latitude at 121.05°E longitude. Case: Moderate southwest winds. White region indicates concentration less than 0.3 ppm.

breeze and slope winds in the vicinity of mountainous terrain. The vertical motions associated with meso-scale

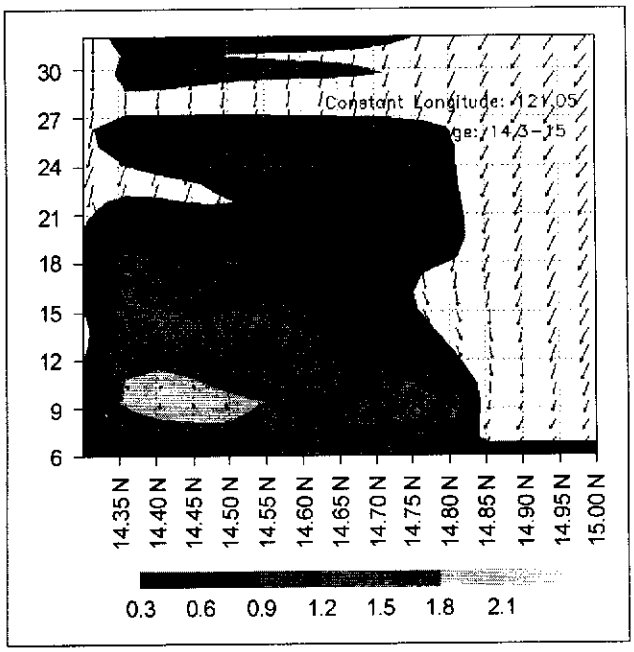

Fig. 25. Hovmoller chart showing the variation of the concentration with time and latitude at 121.05°E longitude. Case: Moderate northeast winds. White region indicates concentration less than 0.3 ppm.

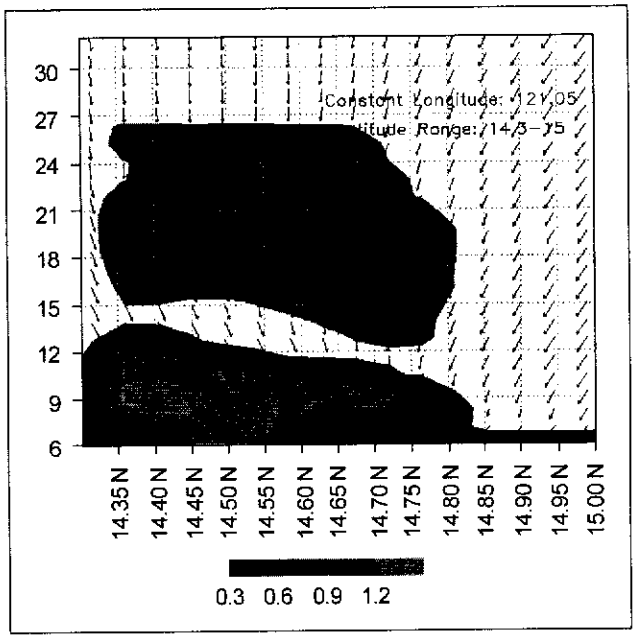

Fig. 26. Hovmoller chart showing the variation of the concentration with time and latitude at 121.05°E longitude. Case: Strong northeast winds. White region indicates concentration less than 0.3 ppm.

circulations result in changes in the inversion height. For example, the inversion height increases in regions of upward meso-scale wind motions. The transport of pollutants by the meso-scale winds also affects the diurnal variations of pollutants.

The effect of cloudiness in ground heating is incorporated in the model through the specification of the total albedo in the prediction of the surface temperature. High albedo values are equivalent to large cloud amounts. In the model simulations, we have arbitrarily adopted the following correspondence between albedo and cloudiness: 40% as partly cloudy, 70% as cloudy, and 90% as overcast. In the simulation for the control case, we specified an albedo of 40%, which is equivalent to a partly cloudy sky condition. Therefore, to determine the effect of cloudiness, we compared the simulations for cloudy skies and overcast skies with those of the control case.

The pollution concentration patterns for the cloudy and overcast cases are shown in Figs. 27 to 30. For the cloudy case in Fig. 28, a fairly complicated longitudinal variation can be observed. In the extreme western sections, only a maximum which occurs in the morning is seen. The evening maximum was not able to develop because of the transport of non-polluted air from Manila Bay. In the eastern sections where the effect of transport is weak, the morning maximum tends to persist throughout the entire day. Note, however, that there is a strong evening maximum near the easternmost section.

The tendency of occurrence of only a morning maximum is also seen in the latitudinal variation for the cloudy case (Fig. 30). A deviation from this tendency is seen near 14.7°N where a small section with an evening maximum is observed. In the case of overcast skies (Figs. 27 & 29), the only appreciable maximum occurs in the evening. This occurs because the positive contribution of the pollution source is larger than the negative contribution of the sink during the daytime; hence, the concentration progressively increases with time. During the hours that follow, the effect of the sink finally overcomes the pollution source. Therefore, the concentration subsequently decreases with time.

Effect of inversion height and inversion strength

We end the discussion of the dependence of the diurnal variation on the prevailing atmospheric conditions by

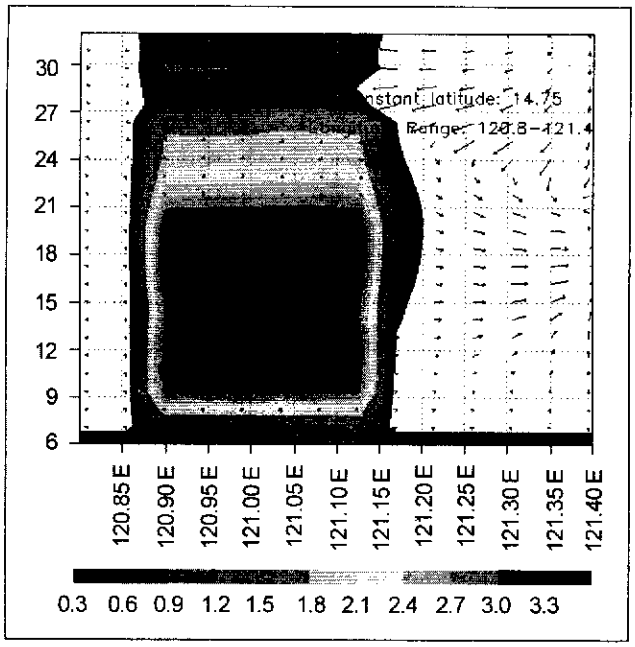

Fig. 27. Hovmoller chart showing the variation of the concentration with time and longitude at 14.75°N latitude. Case: Overcast. White region indicates concentration less than 0.3 ppm.

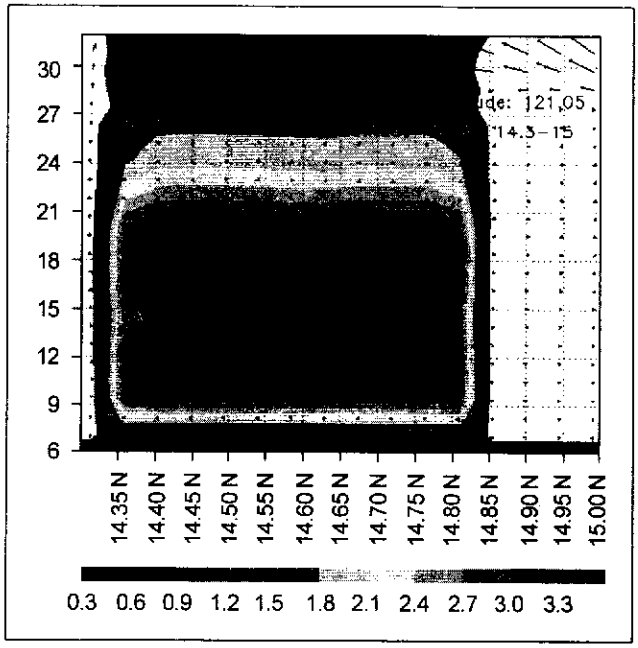

Fig. 29. Hovmoller chart showing the variation of the concentration with time and latitude at 121.05°E longitude. Case: Overcast. White region indicates concentration less than 0.3 ppm.

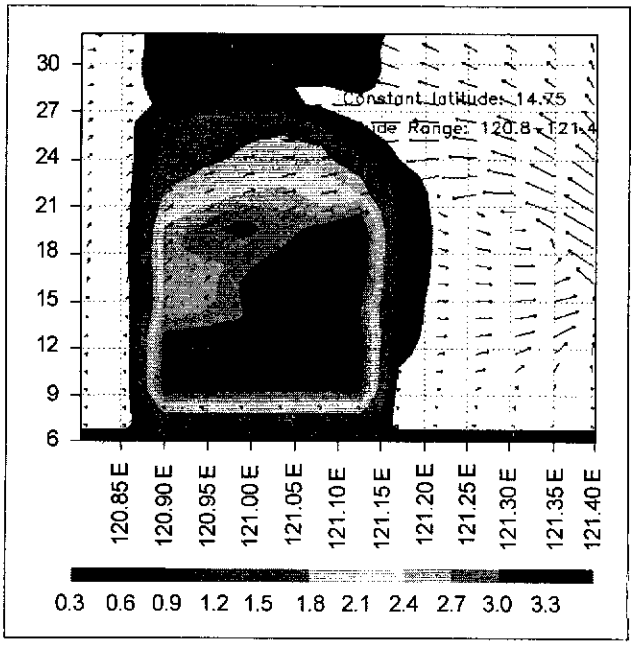

Fig. 28. Hovmoller chart showing the variation of the concentration with time and longitude at 14.75°N latitude. Case: Cloudy skies. White region indicates concentration less than 0.3 ppm.

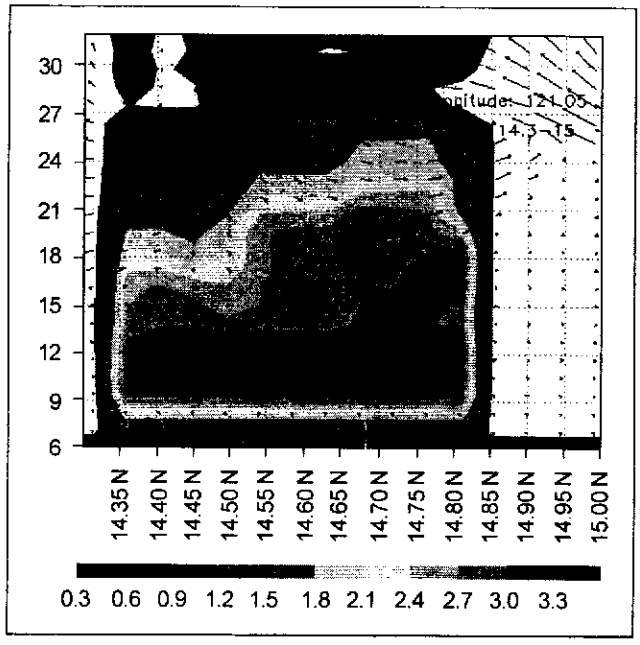

Fig. 30. Hovmoller chart showing the variation of the concentration with time and latitude at 121.05°E longitude. Case: Cloudy skies. White region indicates concentration less than 0.3 ppm.

analyzing the effect of the stability of the atmosphere. The stability considered here refers to the tendency of perturbations along the vertical direction to amplify or dissipate due to the effect of buoyancy. The occurrence

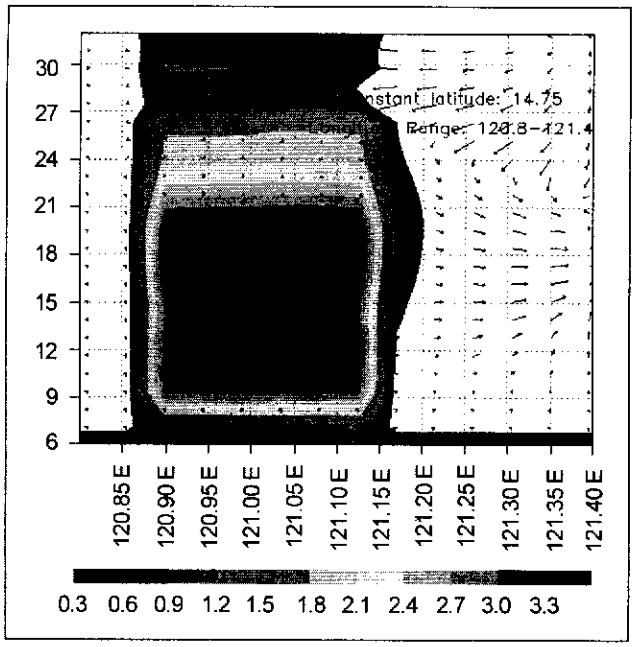

Fig. 27. Hovmoller chart showing the variation of the concentration with time and longitude at 14.75°N latitude. Case: Overcast. White region indicates concentration less than 0.3 ppm.

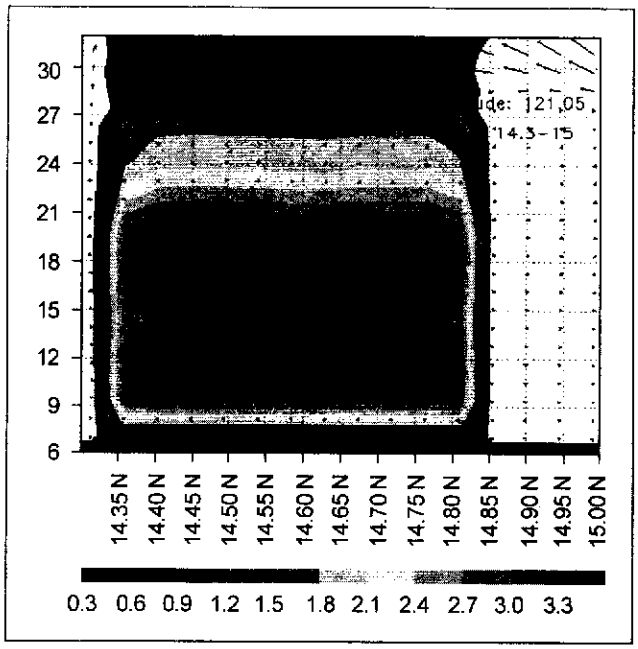

Fig. 29. Hovmoller chart showing the variation of the concentration with time and latitude at 121.05°E longitude. Case: Overcast. White region indicates concentration less than 0.3 ppm.

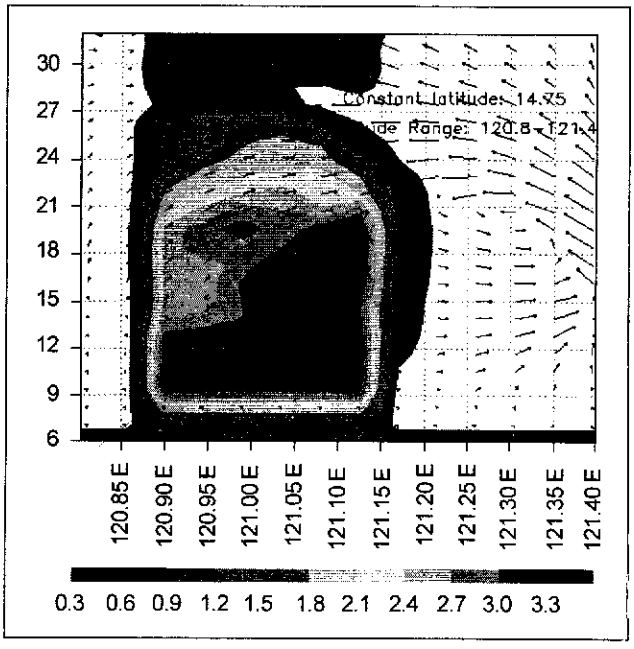

Fig. 28. Hovmoller chart showing the variation of the concentration with time and longitude at 14.75°N latitude. Case: Cloudy skies. White region indicates concentration less than 0.3 ppm.

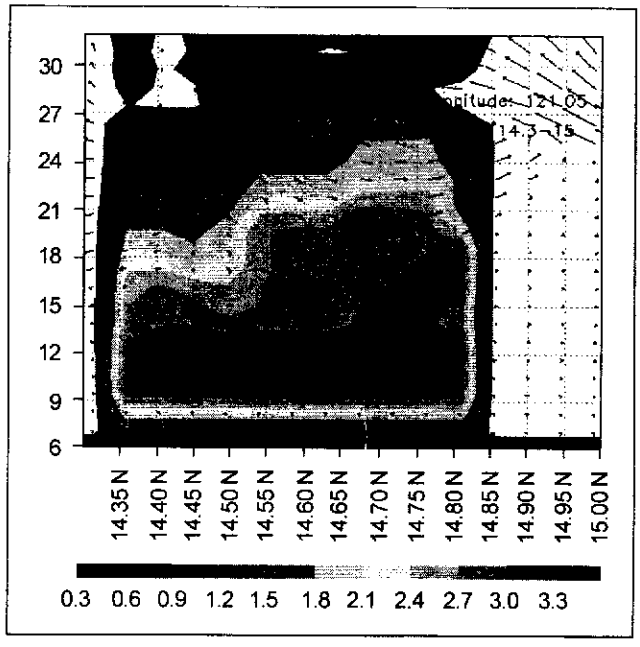

Fig. 30. Hovmoller chart showing the variation of the concentration with time and latitude at 121.05°E longitude. Case: Cloudy skies. White region indicates concentration less than 0.3 ppm.

analyzing the effect of the stability of the atmosphere. The stability considered here refers to the tendency of perturbations along the vertical direction to amplify or dissipate due to the effect of buoyancy. The occurrence

of buoyancy is indicated by the vertical temperature distribution of the atmosphere. During the early morning hours, the lowest layer of the atmosphere is usually characterized by an increase in temperature with height; this layer is the so-called "ground inversion layer". Due to the increase of temperature with height, the ground inversion layer is very stable with respect to perturbations in the vertical velocity. Hence, the vertical mixing of pollutants and other atmospheric processes are minimized. Above the inversion layer, the temperature normally decreases with height until the tropopause. This portion of the atmosphere is also stable but less stable than the underlying ground inversion layer. The thickness of the ground inversion layer and the rate of increase of temperature with height (or inversion strength) are important parameters which control the mixing of pollutants. A strong inversion indicates a very stable atmosphere. The top of the inversion layer is essentially a lid, which prevents the upward transport of pollutants to the overlying atmospheric layers.

The early morning values of the two parameters, the strength and the height of the inversion, involving the temperature profile described above are important in controlling the subsequent daytime increase in the inversion height. This increase is primarily a result of the solar heating of the ground. It is, therefore, necessary to incorporate these two parameters in the mixed layer model. We incorporated these parameters by means of the height of the mixed layer (Z_T) and the temperature difference indicated by the quantity DTN in Fig. 6. The quantity DTN incorporates approximately the effect of the strength of the ground inversion in the mixed layer model. We then investigated the dependence of the diurnal variation of concentration on the strength and height of inversion by doing simulations with different initial values of these two parameters.

We discuss first the dependence of the diurnal variation of the pollution concentration on the height of the inversion or the mixed layer. Two values of the inversion height are considered: 300 m and 500 m. The simulations using these values are shown by the Hovmoller charts in Figs. 31 to 34. The patterns in these charts were compared with those of the control run which used an inversion height of 200 m. Comparison of the control run and the simulation runs show that semi-diurnal variation occurs for all values of the inversion height.

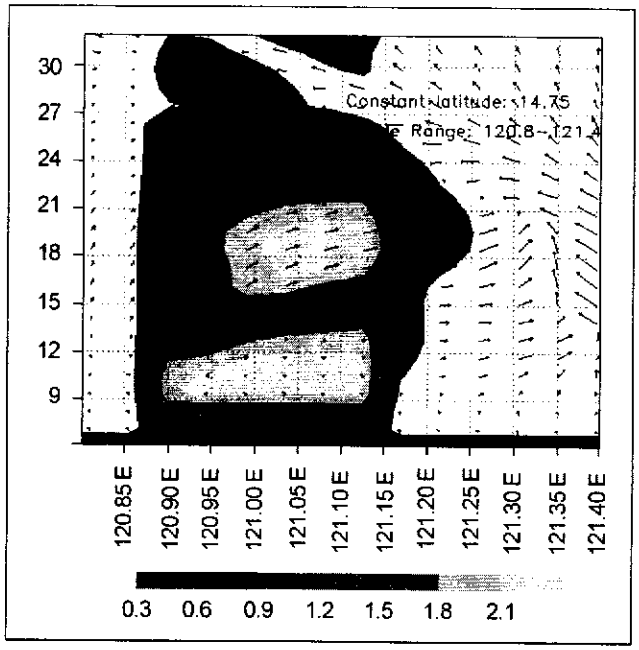

Fig. 31. Hovmoller chart showing the variation of the concentration with time and longitude at 14.75°N latitude. Case: Inversion height of 300 m. White region indicates concentration less than 0.3 ppm.

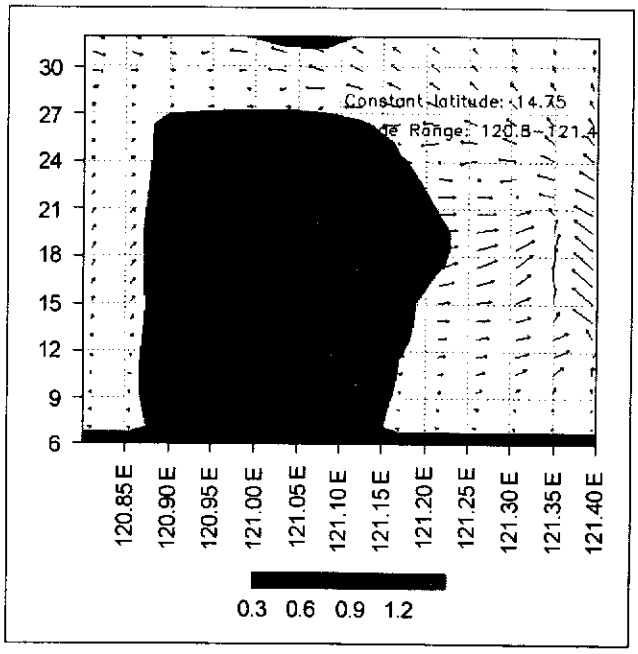

Fig. 32. Hovmoller chart showing the variation of the concentration with time and longitude at 14.75°N latitude. Case: Inversion height of 500 m. White region indicates concentration less than 0.3 ppm.

In all diagrams, it can be observed that the morning maximum is well-defined in all sectors of Metro Manila.

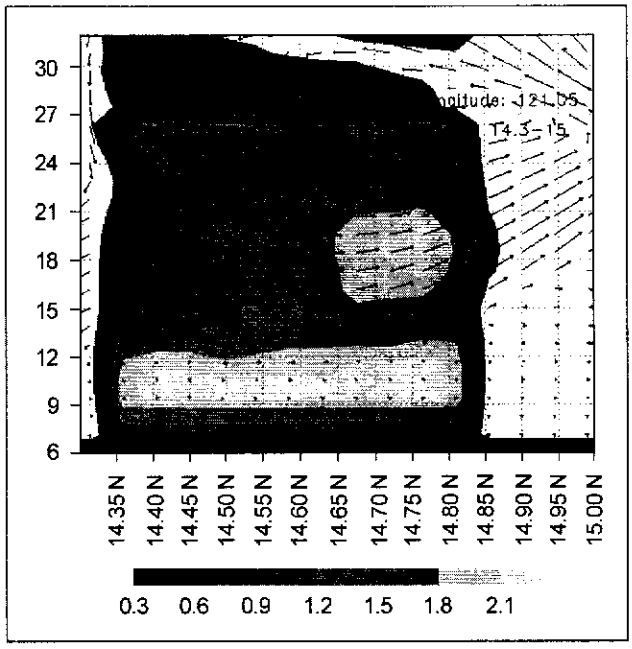

Fig. 33. Hovmoller chart showing the variation of the concentration with time and latitude at 121.05°E longitude. Case: Inversion height of 300 m. White region indicates concentration less than 0.3 ppm.

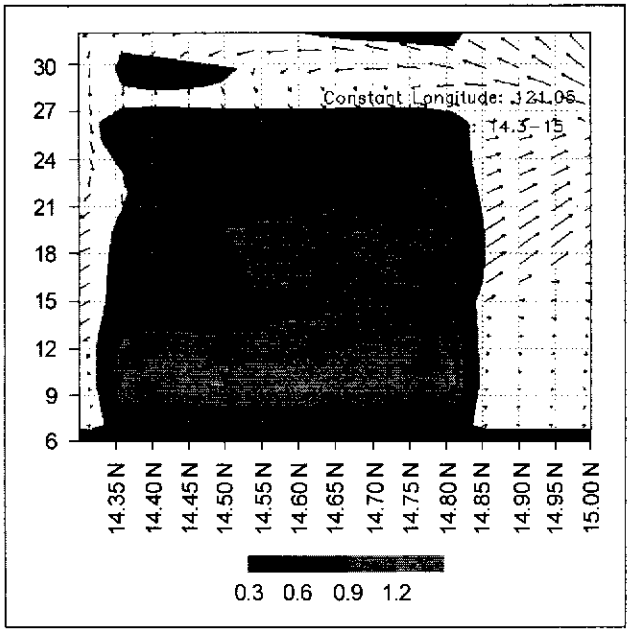

Fig. 34. Hovmoller chart showing the variation of the concentration with time and latitude at 121.05°E longitude. Case: Inversion height of 500 m. White region indicates concentration less than 0.3 ppm.

In contrast, the evening maximum tends to be weak over the southwest sectors; the highest values of the maximum are found over the northeastern sectors. The shape of the time variation is basically unchanged. However, the amplitude of the variation is strongly affected by the change in height. As expected, based on the source term in Eq. (1), we find the concentration values in Figs. 31 to 34 to be inversely proportional to the height of inversion. Based on the maximum values in the diagrams, we see the following correspondence between concentration and inversion height: 3.3 ppm (200 m); 2.1 ppm (300 m); and 1.2 ppm (500 m).

To determine the dependence of the concentration on the strength of the inversion (as specified by values of DTN), several simulations were made. The values range from DTN = 1 (control case) to 5. Very little dependence of the diurnal variation on the strength of inversion is observed as evidenced by comparison of the diurnal variations in Figs. 35 & 36 (DTN = 5) with those of Figs. 17 & 18 (control case). The similarities in the concentration patterns for the two cases may be explained by the fact that the solar heating of the ground in both cases is relatively intense. The ground is sufficiently warm in both cases; thus, the variations in the inversion height are essentially the same for both. In order to verify this explanation, a simulation was made for which DTN is set equal to 5, while the sky condition is specified as overcast. The Hovmoller charts for this simulation are shown in Figs. 37 & 38. The conditions used in this simulation is exactly the same as those in Figs. 35 & 36, except for the difference in sky condition. In Figs. 35 & 36, the sky condition is partly cloudy. In contrast, the sky condition for Figs. 37 & 38 is overcast so that the solar heating of the ground is negligible. Hence, there is no significant increase in the height of the inversion.

Comparing the two sets of Hovmoller charts for the partly cloudy and overcast cases, we note the large difference in the concentration patterns. The overcast simulation is characterized by large values of concentration during the daytime. In addition, the time variation has substantially only one maximum that occurs at about 6:00 P.M, which is in contrast with the two maxima found in Figs. 35 & 36 for the partly cloudy case. In the case of overcast skies, the concentration increases until it reaches the 6:00 P.M. maximum. Thereafter, the concentration decreases with time due primarily to the decrease in the intensity of the source.

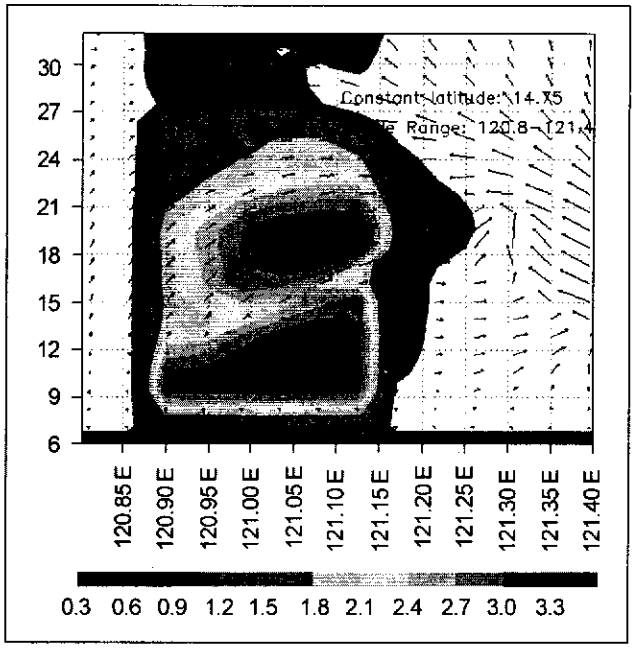

Fig. 35. Hovmoller chart showing the variation of the concentration with time and longitude at 14.75°N latitude. Case: Inversion strength of 5 degrees and partly cloudy skies. White region indicates concentration less than 0.3 ppm.

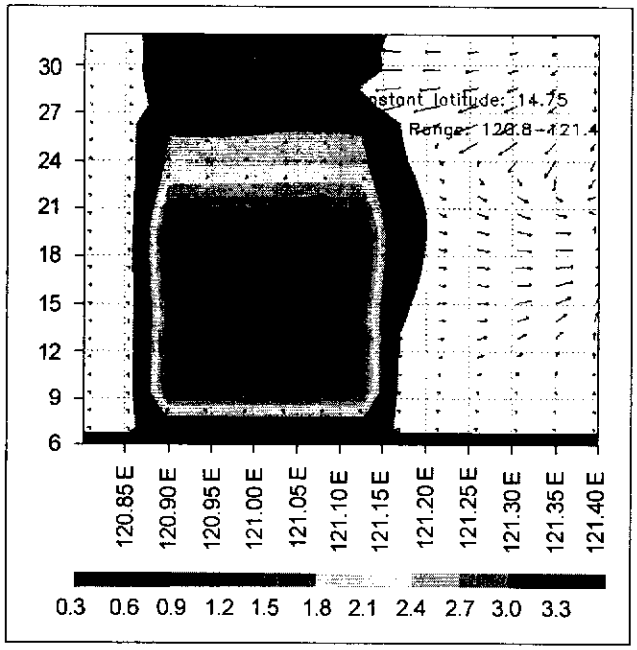

Fig. 37. Hovmoller chart showing the variation of the concentration with time and longitude at 14.75°N latitude. Case: Inversion strength of 5 degrees and overcast skies. White region indicates concentration less than 0.3 ppm.

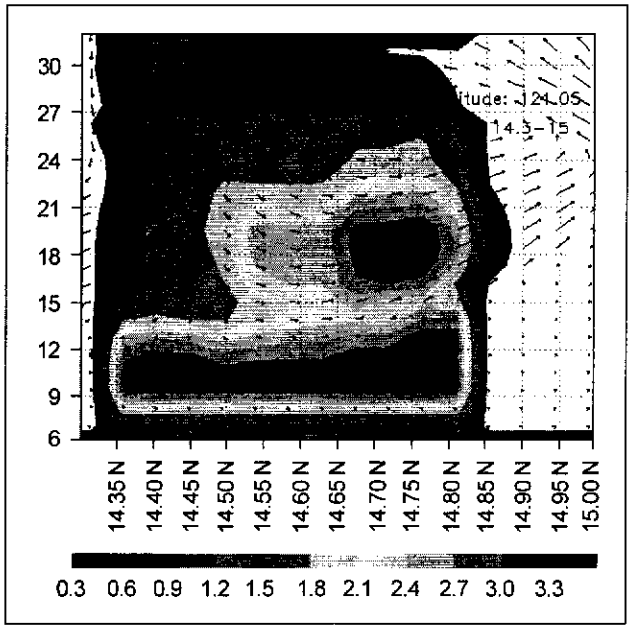

Fig. 36. Hovmoller chart showing the variation of the concentration with time and latitude at 121.05°E longitude. Case: Inversion strength of 5 degrees and partly cloudy skies. White region indicates concentration less than 0.3 ppm.

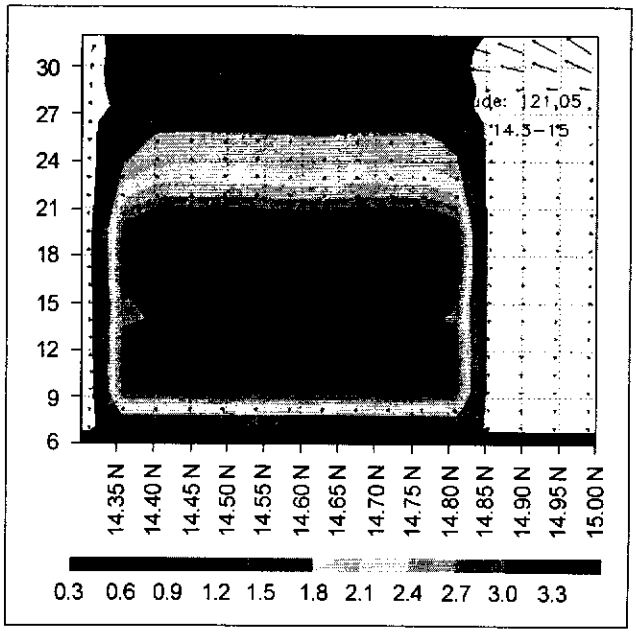

Fig. 38. Hovmoller chart showing the variation of the concentration with time and latitude at 121.05°E longitude. Case: Inversion strength of 5 degrees and overcast skies. White region indicates concentration less than 0.3 ppm.

As a summary of the simulations, we note that the time variation of the pollution concentration during the day is influenced significantly by the prevailing wind and the sky condition, as well as the height and the strength

of the inversion in the morning. Large variations can occur, depending on the values of these parameters. Nevertheless, there is one type of variation which occurs in almost all of the simulations. This variation is characterized by two maxima: one occurs in the morning, while the other occurs in the evening. This semi-diurnal variation is best defined over the northeastern sectors of Metro Manila. We note that the strong tendency in the simulations to exhibit a semi-diurnal variation is in agreement with the three-year average observations of Valeroso et al. (1996).

SUMMARY AND CONCLUSIONS

This paper describes a theoretical study of the diurnal variations of air pollution over Metro Manila. The purpose of the study is to determine the dependence of the diurnal variations on the characteristics of the prevailing atmospheric conditions. The different conditions or parameters which are considered are wind speed, wind direction, cloudiness, and thermal stratification of the atmospheric layer near the ground. In order to determine the effects of these parameters on diurnal variation, we compared the results of the simulation runs having these parameters against those of a control experiment. The control experiment corresponds to a case for which the following assumptions in the initial conditions were made: wind is essentially calm; sky is partly cloudy; height of the inversion is 200 m; and inversion strength is weak (1°C).

The simulations for the control case show a predominant tendency for the concentration to vary semi-diurnally with a morning, as well as an evening, maximum. These two maxima are generally separated by a near noontime minimum, which results primarily because of the large values of the inversion height at this time of the day. The amplitude of the variations tends to be largest over the northeastern sections of Metro Manila.

In general, moderate to strong prevailing winds do not change the semi-diurnal characteristic of the concentration variations. However, strong winds decrease the amplitude of the variations. Moreover, the morning maxima tend to be relatively strong over the eastern sections of Metro Manila when the prevailing wind is northeastward; the reverse happens when the wind is southwestward.

Cloudy skies increase the concentration of pollutants. In addition, cloudy skies tend to decrease the area affected by the evening maximum. When the sky is overcast, the semi-diurnal variation with two maxima degenerates into a single maximum that occurs in the evening.

The results of the simulations for determining the effect of the stability of the atmosphere with respect to vertical mixing are in agreement with expectations. A highly stable atmosphere (small inversion height and strong inversion) results in high pollutant concentrations. In general, a semi-diurnal variation also tends to prevail. The exception to this prevalence occurs when the inversion is strong and is accompanied by an overcast condition. This extremely stable condition results in the suppression of the morning maximum and the existence of only the evening maximum.

REFERENCES

Barkan, J. & Y. Felicks, 1993. Observations of the diurnal oscillation of the inversion over the Israel coast. *Boundary-layer meteor.* 62: 393-409.

Deardorff, J.W., 1978. Efficient prediction of ground temperature and moisture with inclusion of a layer of vegetation. *J. Geophys. Res.* 83: 1889-1903.

Estoque, M. A. & K. Ninomiya, 1976. Numerical simulation of Japan Sea effect snowfall. *Tellus.* 28: 243-253.

Garcia, B.A., et. al., 1988. Concentrations, sources, and particle size distribution of the atmospheric aerosol of the Oviedo Urban Nucleus (Spain). *Atm. Environ.* 22 (12): 2963-2969.

Glendening, J.W., 1990. A mixed layer simulation of daytime boundary layer variations within the Los Angeles basin. *Mon.Wea. Rev.* 118: 1531-1550.

Heinsohn, R.J. & R.L. Kabel, 1999: Sources and control of air pollution. New Jersey, Prentice Hall, Inc.: 696 pp.

Kerdar, A.S., 1996. An urban air quality diffusion model (doctorate thesis). University of the Philippines. 252 pp.

Keyser, D. & R.A. Anthes, 1977. The applicability of a mixed layer model of the planetary boundary layer to real data forecasting. *Mon. Wea. Rev.* 105: 1351-1371.

Lavoie, R.L., 1972. A meso-scale numerical model of lake effect storms. *J. Atmos. Sci.* 29: 1025-1040.

Leighton, P.A., 1961. Photochemistry of air pollution. New York, Academic Press: 300 pp.

Nazaroff, W.W. & L. Alvarez-Cohen, 2000. Environmental engineering science. New York, John Wiley and Sons: 690 pp.

Tubal, G.B., 2001. Diurnal variations of the convective boundary layer height over Metro Manila, Philippines and its effect on pollutant concentration (dissertation). University of the Philippines, Diliman.

Valeroso, I., C.A. Monteverde, & M.A. Estoque, 1992. Diurnal variations of air pollution over Metro Manila. *Atmosfera.* 5: 241-258.

Date received: December 19, 2002
Date accepted: March 18, 2003